Structural properties of a chain of dust particles in a field of external forces

A. V. Fedoseev,[1,*] M. V. Salnikov,[2] M. M. Vasiliev,[1] and O. F. Petrov[1]
[1]*Joint Institute for High Temperatures RAS, Moscow 125412, Russia*
[2]*Institute of Thermophysics SB RAS, Novosibirsk 630090, Russia*

(Received 25 May 2022; revised 14 July 2022; accepted 2 August 2022; published 25 August 2022)

This paper presents a numerical study of the structural parameters of a one-dimensional chain of three dust particles levitating in the near-electrode layer of an rf discharge or in the stratum of a dc discharge. The model considers the motion of dust particles under the action of gravity, external electric field, the Coulomb repulsion, and the electrostatic force from the space charge surrounding the dust particles. Particular attention is paid to the effect of plasma polarization around dust particles and the wake formation under the action of the external electric field. Calculations showed that the charge of the first dust particle in the chain and the total charge of the entire chain, as well as the length of the chain, grow linearly with the external electric field strength. Obtained data are in qualitative agreement with the experimental and numerical data presented in the literature. It was shown that for a certain large value of the external electric field, the charge of the third dust particle is the smallest of all the particles in the chain. It was found that with an increase in the mean value of the external electric field, the chain of dust particles is displaced as a whole in the direction opposite to the action of the electrostatic force on them.

DOI: 10.1103/PhysRevE.106.025204

I. INTRODUCTION

The formation of the ordered structures of dust particles in low-temperature laboratory plasmas is a widespread and highly intriguing phenomenon [1–5]. Self-organized dust structures can be easily obtained in laboratory conditions in rf discharges [1–3] and dc discharges [4,5], in which charged dust particles are trapped in electric fields. Along with well-known two-dimensional (2D) crystals of dust particles levitating above the lower electrode, one-dimensional (1D) chains of dust particles were also obtained in different investigations [4–13]. Various mechanisms have been proposed for the interaction of dust particles with each other and for the dust particles' alignment into linear chains or strings [6,10,14–16]. It should be emphasized that a one-dimensional dust particle chain is a simple example for studying one-dimensional particles' interaction, momentum and energy transfers, phase transitions, and wave propagation.

Along with the works mentioned above, a cycle of works on the formation of chains of dust particles in the Plasma Kristall-4 facility should also be noted [8,17–20]. A series of works on the experimental observation of long vertical chains of dust particles trapped inside a glass box placed on the bottom electrode of an rf discharge [21–26] should also be mentioned. In [26] linear chains of one to seven dust particles long were obtained in such a discharge. The interparticle distances in such chains were measured and the charges of each dust particle were calculated numerically.

The most common numerical model for studying clusters and chains of dust particles today is a DiP3D model based on the Particle-in-cell (PIC) method [27–30]. In recent papers, a three-dimensional DiP3D model has been presented, in which the calculation of plasma flow around the structures of dust particles is performed. DiP3D makes it possible to self-consistently calculate the charges of dust particles, take into account elastic and inelastic collisions of electrons and ions with neutral atoms, and even allow calculations taking into account the magnetic field [30]. Using the referred model, the charges of dust particles and the interparticle distances in the dust chain were calculated for subsonic and supersonic regimes of plasma flow. The disadvantages of the DiP3D include numerical complexity and the inability to obtain accurate solutions in the plasma region closest to the dust particles. On the basis of the PIC method, a complex model Particle-in-cell Monte Carlo collision/particle-particle particle-mesh was also created and tested, in which, around a stationary cluster of dust particles [31], the kinetics of ions and electrons is simulated. This model simulates with good accuracy the process of dust particles charging in a cluster. However, its complexity [joint solution by two methods: PIC far from the dust particles and molecular dynamics (MD) near the dust particles] does not allow to independently model the self-consistent formation of a dust structure.

Modeling the arrangement of dust particles in the chains was also considered in [18,25,32]. Within the framework of these papers, the DRIAD (dynamic response of ions and dust) model was presented, in which, using the MAD (molecular asymmetric dynamics) approximation, the simultaneous motion of ions and dust particles was simulated, where the time steps for dust particles and ions are different. In [32], the motion of two dust particles in an external ion flow was simulated and it was demonstrated that the dust particle located downstream of the ion flow discharges relative to the dust particle located upstream. In [25], numerical studies of a chain of seven dust particles were carried out for three configurations of the spatial (vertical) electric field distributions: constant, linear, and quadratic. The work [18] investigated

*alex.fed245@gmail.com

configurations of many dust particles and compared them with the results of an experiment performed within the framework of the Plasma Kristall-4 Project. The main disadvantage of this model is its high computational power requirements for calculating large configurations of dust particles, and exposure to computational noise during charging of dust particles [32]. This computational noise also does not allow one to calculate with high accuracy the spatial distribution of the plasma potential in the vicinity of the dust particles [18].

In this paper, a numerical model for studying the structural properties of a one-dimensional dust particles chain is presented. The results consist of a self-consistent calculation of the dust particle charges and interparticle distances depending on the configuration of the external electric field.

II. MODEL

The presented model considers the self-consistent spatial ordering of a one-dimensional dust particle chain under the action of various forces. It also takes into account the dust particles charging self-consistently. The forces under consideration are Coulomb interaction (repulsion) force between the particles, the gravity force, and the electrostatic force from an external electric field, as well as the force acting on each dust particle from the plasma space charge (of ions and electrons). The presented model can be conditionally divided into two main blocks. Block 1 calculates the self-consistent spatial distributions of the space charge $n(\boldsymbol{r})$ and the plasma potential $U(\boldsymbol{r})$ around a stationary dust particle chain (the positions of dust particles r_k are calculated prior and do not change). Block 1 also calculates the self-consistent charges of these dust particles Q_k. In block 2, the calculations of equilibrium positions of each dust particle are carried out, taking into account the spatial distribution of the plasma potential and the dust particle charges obtained in the framework of block 1.

The computational domain is chosen as a parallelepiped with sides L_x, L_y, L_z, where x, y, z are the Cartesian coordinates (see Fig. 1). In this paper, the one-dimensional chain of three dust particles placed on the z axis ($x = y = 0$) is considered. The chain is oriented in the direction of the external electric field $\boldsymbol{E} = (0, 0, E)$ and the gravitational field $\boldsymbol{g} = (0, 0, g)$. Therefore, the size of the computational domain along the z axis is chosen to be three times larger than in the transverse directions, $L_x = L_y \ll L_z$. With the presented configuration, the problem becomes cylindrically symmetric, and the forces acting on the dust particles in the direction of the x and y axes prove to be symmetrical around the z axis. Spatial distributions of the space charge $n(x, y, z)$ and the plasma potential $U(x, y, z)$ are also axisymmetric and, thus, are defined as functions $n(\rho, z)$ and $U(\rho, z)$.

In this work, the following dimensionless quantities are used. All variables which denote length are normalized to the ion Debye length $\lambda_i = \sqrt{kT_i/4\pi e^2 n_0}$, where n_0 is the unperturbed plasma density far from the dust particle chain. The value n_0 is chosen as a normalization parameter for the ion n_i and electron n_e densities. All variables which denote energy are normalized to the ion thermal energy $k_B T_i$, velocity variables are normalized to the ion thermal velocity $V_{Ti} = \sqrt{k_B T_i/m_i}$, and time variables are normalized to λ_i/V_{T_i}. For such a choice of dimensionless variables, the dimensionless

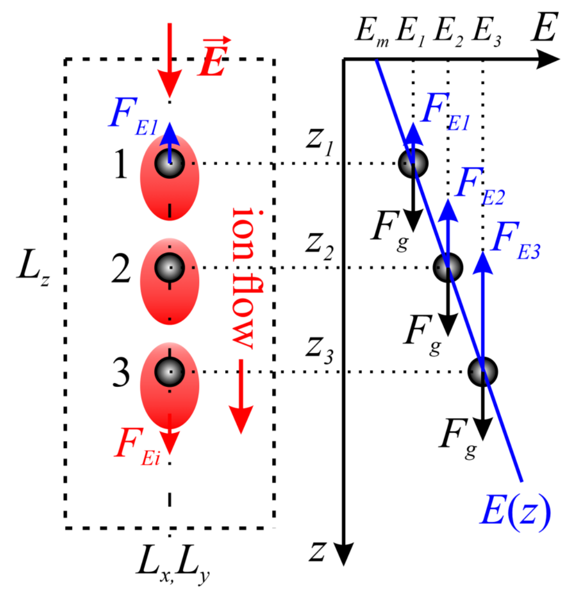

FIG. 1. Schematic representation of the dust particle chain in the computational domain.

forms of the dust particle charge Q' and the external electric field E' are defined as

$$Q' = -\frac{e^2 Z_d}{\lambda_i k T_i}, \quad E' = \frac{eE\lambda_i}{kT_i}. \tag{1}$$

In subsequent descriptions, the dust particle charge and the external electric field strength are considered only as dimensionless quantities. Therefore, for the sake of convenience, the strokes in the notation will be omitted.

In this model, the external electric field spatial distribution $E(z)$ is specified as a linear function of coordinate z:

$$E(z) = E_m + E_k z, \tag{2}$$

where E_m determines the mean value of the electric field strength, and E_k determines the function $E(z)$ slope. Such a linear distribution $E(z)$ was chosen as an approximation for the electric field distribution in the near-electrode layer of an rf discharge, in which the electric field strength increases with approaching the lower electrode [33]. Above the lower electrode of the rf discharge, dust particles usually levitate as a result of balancing of the electrostatic and gravitational forces [34,35]. The same linear dependence can be used as an approximation of the axial electric field spatial distribution in the stratum of a dc discharge, where the electric field strength increases approaching the head of the stratum, over which the dust particles levitate [5,36].

The specified configuration of the electric field strength $E(z)$ corresponds to the stable position of one or more dust particles levitating in the gravitational field [36]. Let us consider one negatively charged dust particle with a charge Q_d, which is in the equilibrium position z_2, where the electrostatic force $F_{E2} = -Q_d E_2$ is balanced by the gravitational force $F_g = mg$, i.e., $F_{E2} + F_g = 0$. When this particle moves down in the direction of the z axis, for example, to position z_3, it will be affected by the electrostatic force $F_{E3} = Q_d E_3$. Since $E_3 > E_2(|F_{E3}| > |F_{E2}|)$, the resulting force will push the dust particle back to the position z_2. Similarly, if the dust particle moves up to the position z_1 with a smaller electric field $E_1 < E_2$, the resulting force will return the dust particle to the equilibrium position z_2.

In the previous version [37] of the model, the self-consistent spatial distribution of the electric potential and the configuration of the dust particle chain were calculated in a constant external electric field, $E(z) = \text{const} = E_m$. The position of the first dust particle of the chain was set to be $z_1 = 0$. In order for dust particles not to scatter from each other, an additional parameter, the external confining force F_{ext}, was introduced. The setup of our model is closer to the real physical situation, when dust particles levitate in an inhomogeneous electric field that counterbalances the gravity. In this case, the equilibrium positions z_k of dust particles in the chain are determined self-consistently, and the parameters of the particle chain (charges and interparticle distances) do not depend on the additional parameter F_{ext}.

In the framework of block 1, the spatial distributions of the space charge and the plasma potential near a fixed chain of dust particles are calculated. At the beginning of the calculations, a set of $\sim 10^6$ ions with a uniform spatial distribution is generated in the computational domain (L_x, L_y, L_z). The initial velocity of each individual ion is determined according to the Maxwellian velocity distribution for the average ion energy corresponding to the temperature $T_i = 273$ K. An isotropic angular distribution of their velocities is specified. Then, the trajectories of these ions according to Newton's motion equations in a three-dimensional space of Cartesian coordinates (x, y, z) are calculated for a constant spatial distribution of the electric potential.

At the initial time, $t = 0$, the total potential spatial distribution is determined analytically as a superposition of the Debye-Hückel potential of three dust particles and the potential of the external electric field:

$$U_{\text{full}}^{0}(\rho, z) = \sum_{k=1}^{N} \frac{Q_k}{r_k} e^{-r_k} - E(z) z,$$
$$r_k^2 = \rho^2 + (z - z_k)^2, \quad \rho^2 = x^2 + y^2, \tag{3}$$

where k is the order number of a dust particle in a chain of N particles, and z_k is the position of the kth dust particle on the z axis.

The ion dynamics in the current model corresponds to the earlier versions [38] of the model. In the course of their movement, ions can collide with a dust particle or with a neutral atom. The average time between ion-atom collisions is determined by the mean free path l_i, which is also a given parameter in the model. The collision of ions with dust particles is determined directly from the calculations of Newton's motion equation for each individual ion. Before the calculation of the plasma parameters spatial distributions, the charges of each dust particle are modified by the following formula:

$$Q_k^{t+1} = Q_k^t + h(I_{i,k} - I_{e,k}), \tag{4}$$

where $I_{i,k}$ is the ion flux to the kth dust particle, calculated from the number of collisions of ions with the dust particle, and $I_{e,k}$ is the electron flux to the kth dust particle, which is determined according to [39].

The ion density spatial distribution $n_i(\rho, z)$ is defined as a quantity directly proportional to the residence time of ions in cylindrical segments of space (ρ, z). The ions' residence time corresponds to the ion density $n_i(\rho, z)$. This correspondence is calculated from the condition that at the boundaries of the system, $n_i(\rho_b, z_b) = n_0 = 1$, based on the previously mentioned nondimensionality criterion. Due to this normalization of the ion density to the constant value n_0 on the region boundaries, the ion motion was calculated for a constant value of the external electric field E_m. It is assumed that the ion flow has sufficient kinetic energy enough for the ions' motion not to be affected by the slope coefficient E_k. The coefficients E_k and E_m are chosen as parameters in the current model, and their dimensionless form is determined in accordance with formula (1).

The electron density spatial distribution $n_e(\rho, z)$ is determined according to the Boltzmann distribution, which is calculated with the current electric potential spatial distribution. Then, the space charge spatial distribution $n(\rho, z)$ is defined as

$$n(\rho, z) = n_i(\rho, z) - n_e(\rho, z). \tag{5}$$

From the obtained space charge spatial distribution $n(\rho, z)$ at the end of each iteration of block 1, a self-consistent plasma potential spatial distribution $U(\rho, z)$ is determined according to the Poisson equation:

$$\Delta U(\rho, z) = -n(\rho, z). \tag{6}$$

This equation is solved using the Jacobi method, which uses a seven-point stencil to represent the discretization of the Laplace operator in a cylindrical coordinate system [40]. It should be stressed that this computational method for solving the Poisson equation for 2D spatial distribution of the electric potential is very suitable for parallel calculations, especially on graphics processing units. The electric potential calculated by (6) modifies the total potential spatial distribution in the computational domain:

$$U_{\text{full}}(\rho, z) = \sum_{k=1}^{N} \frac{Q_k}{r_k} - Ez + U(\rho, z), \tag{7}$$

where r_k is the distance from the point to the kth dust particle.

Block 1 can be represented by an iterative cycle. Its calculation steps are as follows:

(1) The initial positions of dust particles and the initial total potential spatial distribution $U_{\text{full}}^{0}(\rho, z)$ (3) are set. In the computational domain, according to the procedure described above, the coordinates and velocities of the ions are set.

(2) Based on Newton's motion equations, ion trajectories are calculated for the current total potential $U_{\text{full}}^{t}(\rho, z)$.

(3) From the calculated fluxes of ions $I_{i,k}$ and electrons $I_{e,k}$ to the dust particles' surface, the charges of dust particles Q_k (4) are calculated for the next iteration of calculations.

(4) According to the calculated ion trajectories, the ion density spatial distribution $n_i(\rho, z)$ is calculated. Based on the given distribution of the electric potential $U_{\text{full}}^{t}(\rho, z)$, the spatial distribution of the electron density $n_e(\rho, z)$ is calculated, and then the space charge spatial distribution $n(\rho, z)$ is calculated using (5).

(5) A self-consistent plasma potential spatial distribution $U(\rho, z)$ (6) is calculated.

(6) Transition to step 1 for a total potential spatial distribution $U_{\text{full}}^{t+1}(\rho, z)$ (7).

The iterative execution of the block 1 continues until $|U^{t+1}(\rho, z)–U^{t}(\rho, z)| < \varepsilon$ for the whole domain, i.e., when the electric potential in the system stops changing.

Block 2 determines the equilibrium positions of the dust particles according to the forces acting on them. In this model, the influence of the following forces on the dust particles configuration is considered:

(1) Coulomb repulsion force F_q acting on a certain dust particle from all other dust particles.

(2) The gravitational force F_g, which is the same for all particles and is a given parameter.

(3) The force F_n acting on dust particles from the plasma space charge, which is determined according to the obtained potential spatial distribution in block 1.

(4) Force F_E acting on dust particles by an external electric field.

(5) Friction force F_{fr} of a dust particle on neutral gas atoms when moving in the domain.

The sum of these forces determines the total force F_k acting on a single kth dust particle according to the formula (all variables are taken in a dimensionless form):

$$\begin{aligned} F_k &= F_{q,k} + F_{n,k} + F_g + F_{E,k} + F_{fr,k}, \\ F_{q,k} &= \sum_{j\neq k} Q_k Q_j \frac{z_k - z_j}{r^3}, \\ F_{n,k} &= -Q_k \frac{\partial U(\rho, z)}{\partial z}\bigg|_{z=z_k,\rho=0}, \\ F_{E,k} &= \begin{cases} Q_k(E_m + E_k z), z > 0 \\ Q_k E_m, z < 0 \end{cases}, \\ F_{fr,k} &= \gamma \dot{z}_k. \end{aligned} \tag{8}$$

Due to the fact that the mass of dust particles significantly exceeds the mass of ions, the simultaneous calculation of dust particles and ion motion according to Newton's motion equations would take an unlimited time. Therefore, the division of the model into two iterative blocks is utilized. In block 2, it is assumed that the ions are immobile, and the plasma potential spatial distribution $U(\rho, z)$ is constant. In accordance, the motion equations of the dust particles are solved:

$$ma_k = F_k. \tag{9}$$

These equations are calculated in a constant plasma potential spatial distribution until the velocity and acceleration of each dust particle become equal to zero. Such positions of dust particles correspond to equilibrium, at which the total force F_k acting on particle k turns out to be equal to zero.

The considered form of total force (8) is identical to that presented in the DRIAD model [32]. The main difference between these two approaches is in the calculation of force F_n. In [32], F_n is calculated directly from the interaction of a dust particle with each ion. In the case in [32], this force is asymmetric—dust particles act on ions according to the Coulomb potential, and ions interact with a dust particle according to the Debye potential. In the current model, the mean field approximation is considered; i.e., the interaction of dust particles and the surrounding plasma is calculated through the plasma potential spatial distribution, calculated in fixed cells of the computational domain.

Block 2 includes the execution of block 1 for determination of the plasma potential spatial distribution. Thus, the complete algorithm of this model is as follows:

(1) The initial parameters of the dust particle chain are set, namely, the values z_k (dust particle positions) and Q_k (dust particles charges).

(2) Block 1 is executed. If this is the first iteration of block 2, then block 1 is executed from step 0, otherwise from step 1.

(3) Based on the plasma potential spatial distribution calculated by block 1, the equilibrium positions of dust particles are determined using (8) and (9).

(4) Transition to step 1.

Blocks 1 and 2 are executed iteratively until the values of z_k, Q_k, and other spatial distributions of plasma parameters stop changing. This model, despite its apparent simplicity, requires significant computing power. To calculate the trajectories of 10^6 ions as well as the Poisson equation for plasma potential, the GPU architecture is used. However, even with its help, for a chain of three dust particles, the calculation of the steady state condition takes from 10 to 20 days for one mode depending on the magnitude of the external electric field.

III. RESULTS

In the current paper the calculations are carried out for the following parameter values: the dust particle radius $r_0 = 0.01$ and the ion mean free path $l_i = 5$ (in dimensionless units specified in Sec. II). To simulate the dust particle's motion, the functional form (2) of the external electric field $E(z) = E_m + E_k z$ is used. The case of balance between the gravitational force and the electrostatic force (2) acting on a dust particle of a unit dimensionless charge, such that $F_g + F_{Em} = 0$, is considered. It should be noted that the absolute values of these parameters are chosen to be consistent with typical dusty plasma parameters of dc and rf discharges [see, e.g., [41]. The cross section for ion-argon atom charge exchange collisions is taken, and the dimensionless ion mean free path $l_i = 5$ corresponds to the argon pressure $p = 5$ Pa. The dimensionless electric field strength $E = 1$ corresponds to $E = 2.35$ V/cm (i.e., reduced electric field $E/p \sim 63$ V/cm/Torr. The charge number of the micron-sized particle ($r_0 = 1\,\mu$m) is equal to $Z_d = 1650$ for dimensionless charge $Q = 1$.

Figures 2–4 show the spatial distributions of the space charge and plasma potential near a chain of three dust particles. From the two-dimensional representations of these distributions shown in Figs. 2 and 3, it can be seen that the chain shifts as E_m increases, the ion cloud around the chain is significantly warped, and a wake appears downstream of the structure. It is worth noting that Figs. 2 and 3 have been substantially truncated for clarity and ease of presentation. The size of the system for each calculation is chosen in such a way that at the boundaries of the system the plasma turns out to be unperturbed. Figure 4 shows the influence of the mean value of the external electric field strength E_m on the spatial distributions of the space charge $n(\rho, z)$ and the plasma potential $U_{\text{full}}(\rho, z)$ along the dust particle chain. The coefficient E_k of the slope in the electric field spatial distribution (2) is fixed,

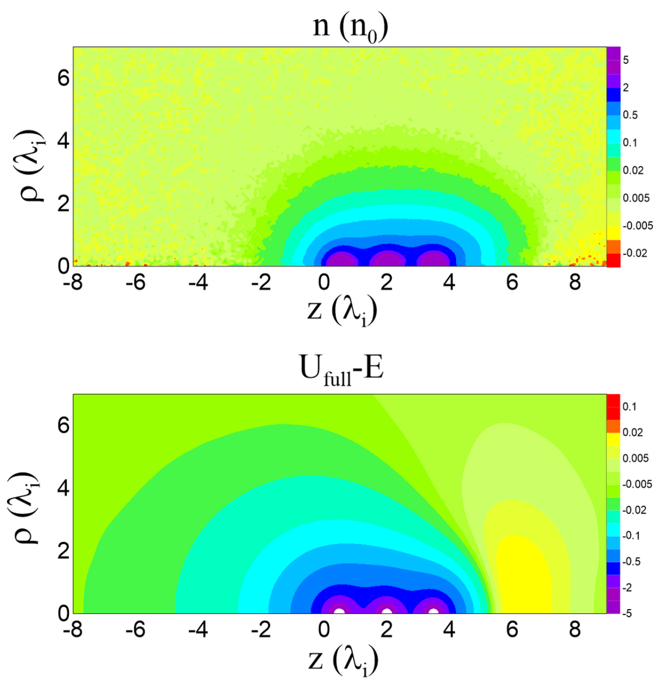

FIG. 2. Spatial distributions of the space charge $n(\rho, z)$ (top) and the total plasma potential $U_{\text{full}}(\rho, z)$–$E(z)$ (down) for $E_m = 0.3$.

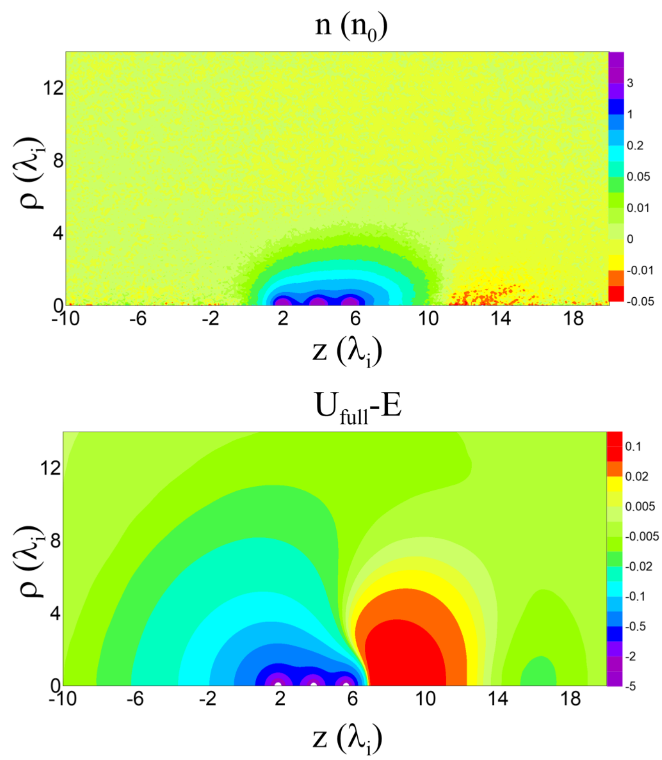

FIG. 3. Spatial distributions of the space charge $n(\rho, z)$ (top) and the total plasma potential $U_{\text{full}}(\rho, z)$–$E(z)$ (down) for $E_m = 1.0$.

$E_k = 0.1$, for the results presented below unless otherwise specified. It is worth noting that the gravitational force F_g acts on the dust particles in the positive direction of the z axis (to the right), while the electrostatic forces $F_{E,k} = E(z_k)Q_k$ act in the negative direction (to the left). With an increase in the strength of the external electric field E_m, the ion cloud around dust particles warps, which is a consequence of the polarization of the ion cloud. This effect is described elsewhere [38] and is intuitively understandable—under the action of a strong external electric field ions are not retained in the particle field. From the basic point of view, it may seem that with an increase in the external electric field strength E_m, the chain of particles should shift towards the action of the electrostatic force on them, $F_{Ek} = Q_k E(z_k)$, i.e., to the left. However, the surprising effect was found that with an increase in the parameter E_m, the dust particle chain shifts as a whole in the direction opposite to the action of the electrostatic force, i.e., in the direction of the gravitational force (to the right). This phenomenon can be explained in terms of the spatial distribution of the plasma potential derivative $F_z(z) = -\frac{\partial U(\rho,z)}{\partial z}|_{\rho=0}$ with respect to the z coordinate, which, when multiplied by the negative charge of the dust particle Q_k, is converted into the force $F_{n,k}$ (8) acting on the dust particles from the plasma space charge.

The spatial distributions of force $F_z(z)$ acting on the probe particle with unit charge $Q = -1$ are shown in Fig. 5. The vertical dashed lines in Fig. 5 show the equilibrium positions z_k of dust particles. The absolute values of the force with which the anisotropic plasma space charge acts on each specific dust particle are determined by the intersection of the dashed lines with the spatial distribution of $F_z(z)$. For the case of an external electric field $E_m = 0.3$, the forces $F_{n,k}$ from the plasma space charge acting on the kth dust particle are $F_{n,1} = 0.55$, $F_{n,2} = 0.26$, $F_{n,3} = -0.23$, while for the case $E_m = 1.0$ they are $F_{n,1} = 0.7$, $F_{n,2} = 0.47$, $F_{n,3} = 0.2$. In the first case, the last (third) dust particle is pushed by the ions to the left, to the side codirectional to the action of the external electric field. In the second case, all three particles are pushed in the direction of gravitational force. In both cases, gravity counterbalances the action of mean electric field E_m. Therefore, without self-consistent changes in the dust particle chain characteristic there should not be any shift. Since the Coulomb repulsive force does not affect the position of the dust particle chain as a whole, it can be concluded that the chain is displaced against the direction of the electrostatic force F_E as a result of the distortion of the ion cloud. This force appears as a result of ion focusing behind dust particles, as described in [27,38,42–46] and others. It has been shown that such distortion leads to the formation of a positive region in the electric potential (see Fig. 6) called a "wake." This remains true in this case as well.

One of the main forces that is usually considered in the ordering of the dust particles in the flowing plasma is the ion drag force [35,39,47–51]. The ion drag force consists of two parts: direct momentum transfer and Coulomb scattering. There are several approximations for the ion drag force for different limits of the ion drift velocities. According to [39], for high values of the ion drift velocity $u_i \gg V_{T_i}$, the ion drag force is mainly determined by the direct momentum transfer and can be described as

$$F_{id} = r_0^2 m_i n_i u_i^2. \tag{10}$$

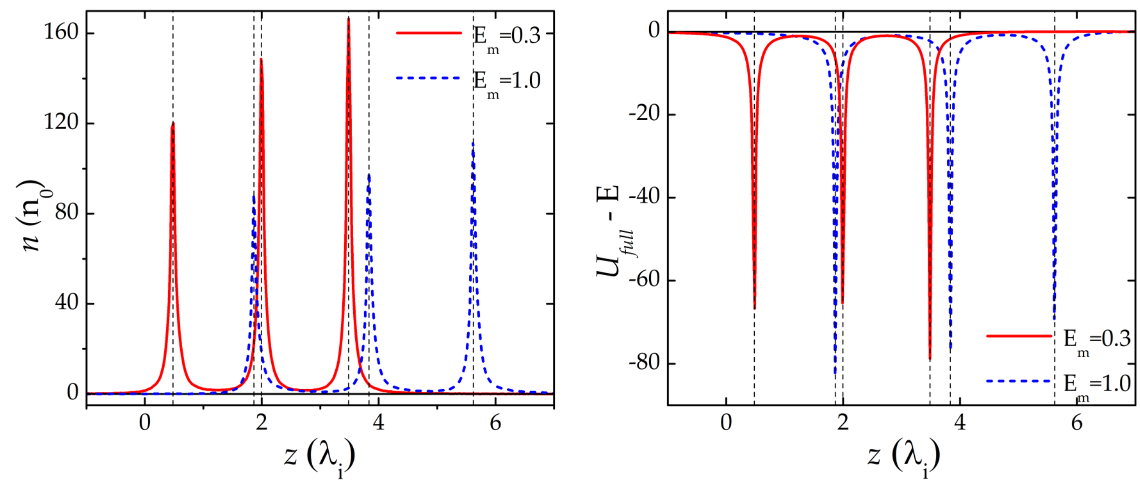

FIG. 4. Spatial distributions of the space charge $n(\rho = 0, z)$ (left) and the total plasma potential $U_{\text{full}}(\rho = 0, z)$–$E(z)$ (right) for various values of the parameter E_m.

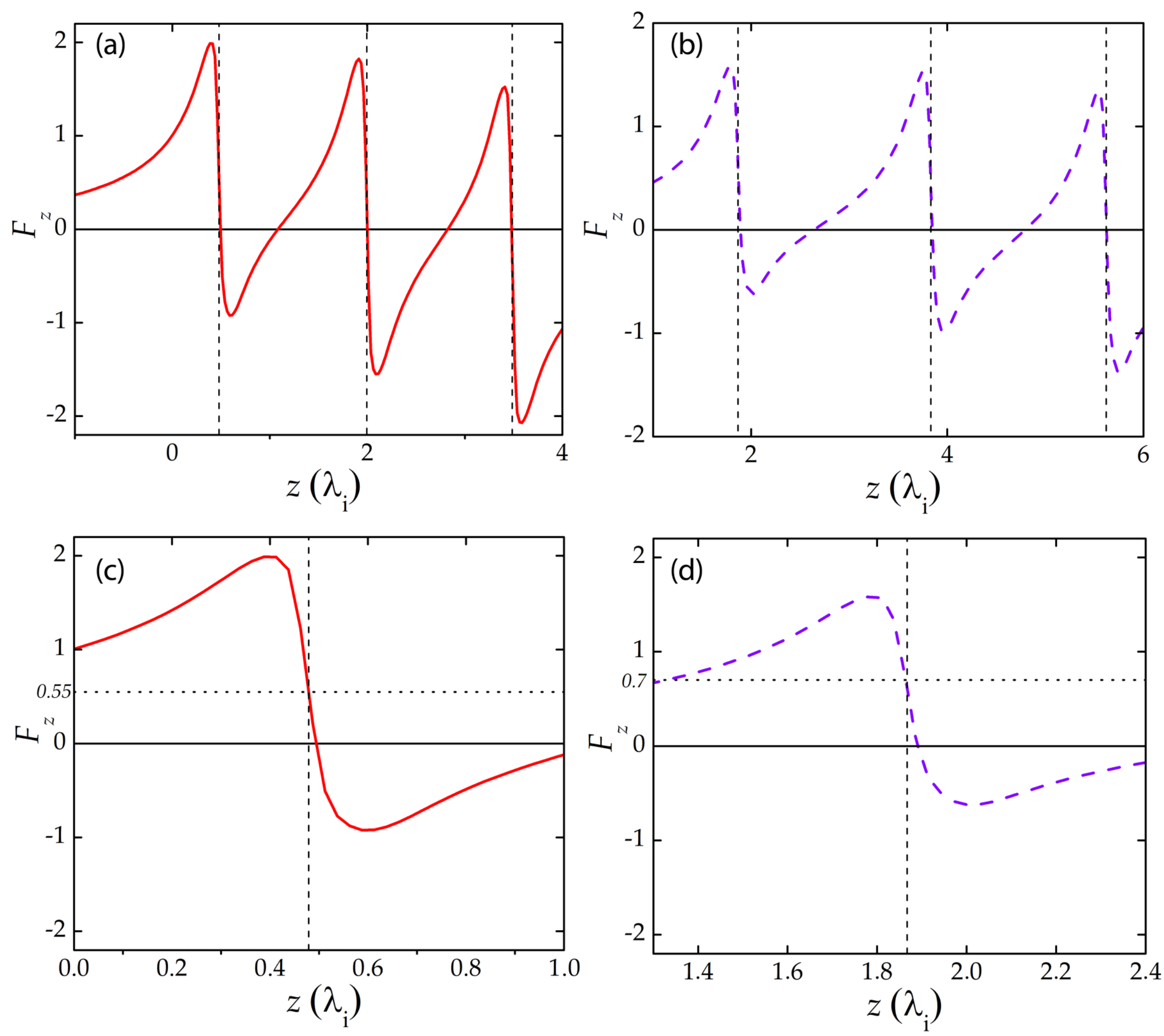

FIG. 5. Spatial distributions of $F_z(z)$ for $E_m = 0.3$ (a), (c) and $E_m = 1.0$ (b), (d). Spatial distributions are presented on two scales: distribution near the entire dust structure (a), (b) and near the first dust particle (c), (d).

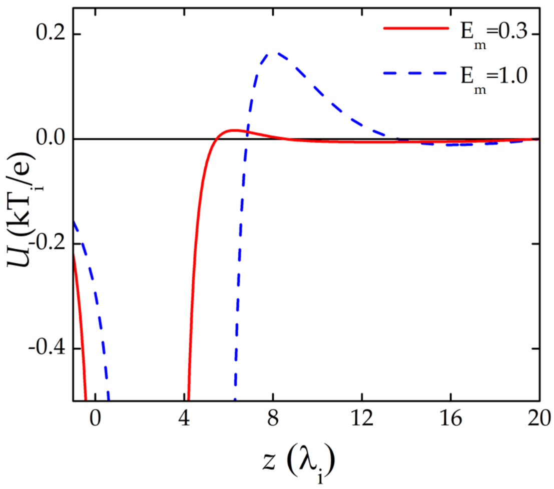

FIG. 6. "Wake" in the plasma potential spatial distribution $U(\rho = 0, z)$ (to the right of the particle chain) for various values of the external field E_m.

For the case of low drift velocity, an approximation presented in [48] is more accurate:

$$F_{id} = \left(\frac{8\sqrt{2\pi}}{3}\right) r_0^2 m_i n_i V_{T_i} u_i \left[1 + \frac{Q}{2}\frac{\lambda_i}{r_0} + \left(\frac{Q}{2}\frac{\lambda_i}{r_0}\right)^2 \Lambda\right], \tag{11}$$

$$\Lambda = 2\int_0^\infty \exp(-x)\ln\left(\frac{2x + Q}{2x\frac{r_0}{\lambda_i} + Q}\right) dx. \tag{12}$$

This force acts on the dust particles in the opposite direction to the force acting from the external electric field:

$$F_{Ef} = Z_n e(E_m + E_k z). \tag{13}$$

Let us compare these forces for two cases, i.e., low value of the dimensionless external electric field $E_m = 0.3$ and high value $E_m = 1$ in the position $z = 0$. According to previous calculations made in [52], the ion drift velocity is $u_i = 0.82\ V_{T_i}$ for $E_m = 0.3$ and $u_i = 2.02\, V_{T_i}$ for $E_m = 1$, correspondingly. The estimations show that the magnitude of the electrostatic force turns out to be $F_{Ef} \sim 1.95 \times 10^{-14}$ and 6.88×10^{-14} N for these cases. The ion drag force estimated by formula (11) turns out to be equal to $F_{id} \sim 1.43 \times 10^{-14}$ and 3.43×10^{-14} N, correspondingly. According to (10), the forces F_{id} are equal to 3.95×10^{-19} and 2.39×10^{-18} N, correspondingly. In both cases the value of the ion drag force calculated by (11) is close to the value of electrostatic force; however, the approximation (11) is less accurate for such drift velocity. In this paper, the ion drag force was not considered due to the difficulties in its implementation but its importance in the ordering of the dust particles into a chain in the flowing plasma should be emphasized. It should also be noted that if the ion drag force would be implemented with approximation (11) it would lead to further shift of the dust particle chain as a whole in the direction of the ion flow, i.e., opposite to the direction of the electrostatic force.

Figure 6 takes a closer look at the potential spatial distribution $U(\rho = 0, z)$. It can be seen that a region with a positive value of the plasma potential appears behind the dust particle chain. These areas represent the main part of the wake, which predictably turn out to be larger for a larger value of E_m. A similar distortion in the potential also occurs between the dust particles, but it does not lead to the appearance of the positive values in the potential as a result of the contribution to the electric potential from the dust particles themselves (see Fig. 4). However, the forces from such space charge distortion indeed act and are shown to be much larger for the larger value of $E_m = 1.0$.

The main goal of this paper is to determine the self-consistent spatial configuration of a chain of dust particles (positions z_k and charges Q_k of each particle, interparticle distances $L_{j,k}$) depending on the external electric field strength. Chain configuration depends on the external forces (gravitational and electric field), on the plasma space charge, and on the Coulomb interaction of the dust particles between each other. The magnitude of Coulomb interaction is determined by the dust particle charges, which, in turn, depend on the external electric field strength and the interparticle distances.

The range of external electric field strengths considered in [37] was significantly limited due to the absence of the gravitational force in the model and the fixed position of the first dust particle. In this paper, a wider range of electric field strengths is considered. Figure 7 shows the dependence of the dust particle charges Q_k on the mean field strength E_m. According to [37,38], the dust particle charge should grow linearly with an increase in the external electric field. In our case, this turns out to be true for the charge Q_1 of the first dust particle in the chain, as well as for the total charge of the entire dust chain $\sum |Q_k|$, the dependence of which on the electric field still remains linear. In experimental studies [53,54], it was shown that the dust particle charges decrease with an increase in number of dust particles. In [27–29,37], it was demonstrated that the second dust particle (downstream of the ion flux) is less charged than the first and third dust particles. Additionally, the charge of the third dust particle turns out to be less than the charge of the first, but greater than the charge of the second dust particle, $|Q_2| < |Q_3| < |Q_1|$. In [16] this phenomenon is defined as fundamental for the formation of a stable structure of the dusty particles, and in [27] it is explained as a result of ion focusing ("lensing"). The results shown in Fig. 7 are broadly consistent with those of the studies mentioned. However, it is worth noting the case of a high electric field strength $E_m = 1.0$, in which the charge of the third dust particle becomes less than the charge of the second one, $|Q_3| < |Q_2| < |Q_1|$. This occurs as a result of the fact that as the field increases, the ion cloud decreases in volume (see Fig. 4), and the ion flow towards the dust chain accelerates. Therefore, shielding of the second dust particle is reduced and its electrostatic lensing becomes significant enough [27] to distort ion trajectories so that the flux to the third dust particle increases. This conclusion is supported by the results of [26], where for a larger number of dust particles, the charge of the third particle also becomes less than the charge of the second one.

It should be noted that during the simulation process, the condition of electrical quasineutrality of the entire computational domain is satisfied; that is, the total charge of the dust chain, shown in Fig. 7(b), is equal to the charge of the plasma

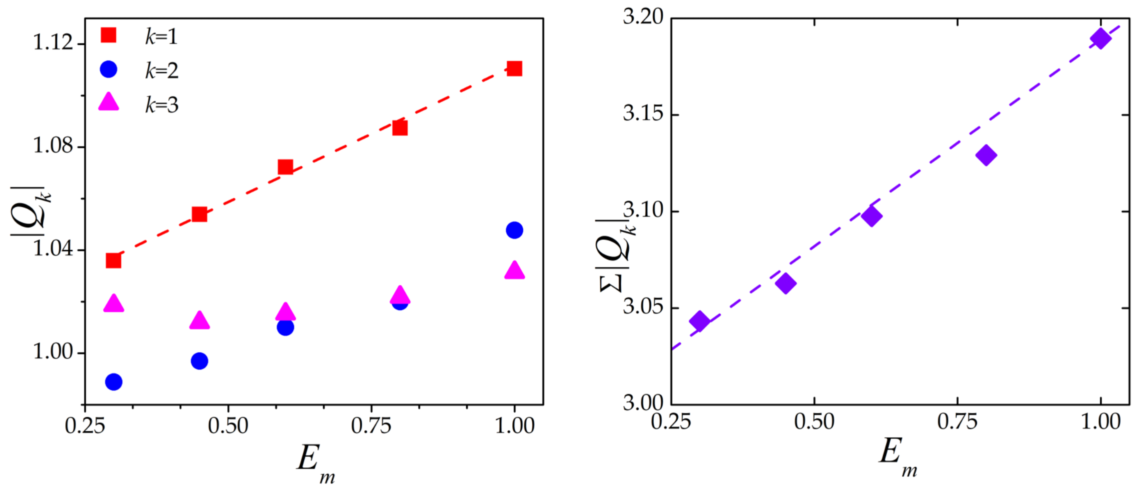

FIG. 7. Dust particle charges Q_k (left) and total charge Q_{sum} of the chain (right) as functions of the dimensionless external electric field E_m.

surrounding it, calculated in dimensionless form by

$$Q_{pl} = \frac{1}{2}\int_{-L_z}^{L_z}\int_{0}^{L_x^2+L_y^2} n(\rho, z)\rho d\rho dz. \tag{14}$$

The total force, which consists of the gravitational force, the external electric field force, the Coulomb force of repulsion of dust particles, and the plasma volume charge force, determines the interparticle distances in the dust particle chain. The dependence of the values of the interparticle distances L_{1-2} and L_{2-3} and the chain length $L_{\text{sum}} = L_{1-3} = L_{1-2} + L_{2-3}$ on the external electric field strength E_m is shown in Fig. 8. The results presented in Fig. 8(a) are in qualitative agreement with the data shown in [37]. A linear increase in the interparticle distances is observed over the entire range of E_m values presented. This growth is explained primarily by an increase in the dust particle charges. Since the total charge of the first and second dust particles (see Fig. 7) is greater than the sum of the charges of the second and third ones, $|Q_1| + |Q_2| > |Q_2| + |Q_3|$, the interparticle distance between the first and second dust particles is greater than that between the second and third, $L_{1-2} > L_{2-3}$. The presence of an asymptote in [37] was explained by the absence of a gravitational force restraining the infinite movement of the chain, as well as by the fixation of the first particle in the chain. In this paper, there is no such asymptote, and the dependences of interparticle distances remain linear, which is more natural. The dependence of the length of the dust chain on the field strength shown in Fig. 8(b) is a direct consequence of the linear growth of the chain total charge. Based on Fig. 8, it can be concluded that with an increase in the external electric field, the chain lengthens, while rearranging in such a way that the interparticle distances are not equal to each other. It should be noted that the inequality of interparticle distances in the dust particle structure is an effect observed both experimentally [25,26] and in numerical simulations [27].

The obtained interparticle distances $L_{1-2} = 150$–$200\,\mu$m and $L_{2-3} = 150$–$180\,\mu$m are in accordance with the experimentally measured ones. Reference [19] presents the results of the PK-4 Project carried out on the International Space Station (ISS), where the stability of a chain of dust particles was studied under zero-gravity conditions. In [19], for a long chain of dust particles of radius $r_0 = 1.7\,\mu$m, it was found that the interparticle distance was close to 250–300 μm for

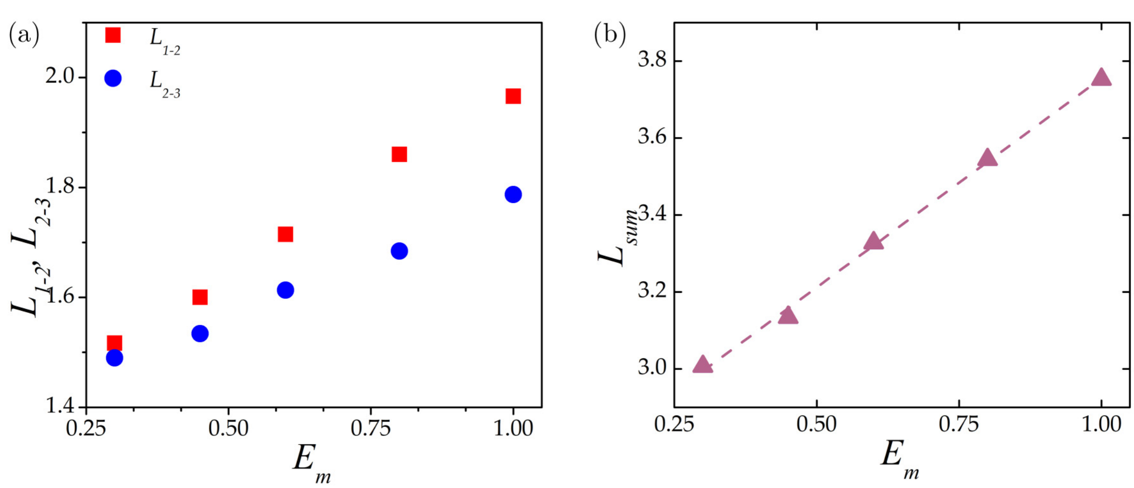

FIG. 8. Dependences of interparticle distances (left) and dust chain length (right) on mean external electric field E_m.

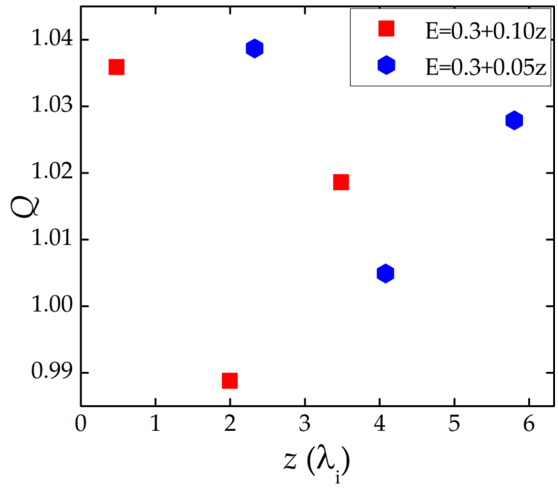

FIG. 9. Distribution of the dust particle charges $Q_k(z)$ in space depending on the slope of the external electric field E_k.

pressure intervals of 25–40 Pa. If we take into account the ratio of the particles' radii in the present calculations and in [19] (assuming the charge of the dust particles is directly proportional to it), then we obtain an appropriate interval of interparticle distances. In [26], the positions of dust particles was experimentally studied under laboratory conditions of rf gas discharge plasma. The dust particles of radius $r_0 = 4.5\,\mu$m were studied at a pressure of approximately 13 Pa. After reaching a steady state, the charge of dust particles in [26] was determined from the iterative calculation. Even when normalized to the radius, the charges obtained in [26] turn out to be 4–5 times greater than the absolute values of the dust particle charges calculated by this model, which is associated with a large value of the external electrostatic field (1100–1350 V/m compared to the maximum of 230 V /m considered in this paper). The experimentally obtained interparticle distances for the case of three dust particles in [26] turn out to be approximately equal to $L_{1-2} \approx 1000\,\mu$m and $L_{2-3} \approx 700\,\mu$m. Considering the ratio of these two quantities, we obtain $L_{1-2}/L_{2-3} \approx 0.7$. In this work, this ratio fluctuates in the interval $L_{1-2}/L_{2-3} \approx 0.85$–1. Thus, despite the differences, the results of the presented model demonstrate acceptable quantitative agreement with experimental data both in laboratory and in zero-gravity conditions.

It is also worth considering the influence of the coefficient E_k [the slope of the function $E(z)$ in formula (2)] on the dust chain structure. Figure 9 shows the space distribution of dust particle charges $Q_k(z)$ depending on the parameter E_k. It can be seen that with an increase in the slope E_k, the electric field displaces the dust chain in the direction of the electrostatic force. In addition, the charge of the central dust particle is reduced by 2%. This is a consequence of the change in interparticle distances, which for the case of $E_k = 0.05$ are $L_{1-2} = 1.75$, $L_{2-3} = 1.72$, and for $E_k = 0.1$ they are $L_{1-2} = 1.52$, $L_{2-3} = 1.49$, which leads to a decrease in the dust particle charges [27,53,54].

IV. CONCLUSION

The behavior of a chain of dust particles placed in gravitational and external electric fields and oriented along them is studied. The investigated situation corresponds to the dust particles' levitation in the near-electrode region of rf discharge or in the stratum of dc discharge, in which the electric field spatial distribution can be approximated by a linear dependence with a certain mean value and slope coefficient.

For this purpose, a numerical model was developed based on simulating the ion motion in an external electric field and the field of negatively charged dust particles screened by the space charge surrounding them. The charges of dust particles were determined self-consistently from the ion and electron flows towards their surfaces, and the positions of the dust particles in the chain were determined taking into account the following forces acting on them: the gravitational force, the electrostatic force from an external electric field, the Coulomb repulsion force, and the electrostatic force from the space charge induced around dust particles.

With the help of numerical simulation, the following surprising effect was obtained and analyzed: With an increase of the external electric field strength, the chain of dust particles shifts as a whole in the direction opposite to the action of the electrostatic force acting on them from the external field, i.e., in the direction of the gravitational force. This occurs even though the ion clouds around the dust particles decrease with increasing electric field due to plasma polarization. The analysis showed that there is a strong force acting on the negatively charged dust particles from the space charge, which arises as a result of ion focusing behind the dust particles in an external electric field. It was also shown that behind the chain of dust particles there is a region with a positive plasma potential (wake), which predictably turns out to be larger for a larger electric field.

The dependences of the dust particle charges and the interparticle distances on the electric field strength were calculated. It was shown that the charge of the first dust particle in the chain, as well as the total charge of the entire chain, increases linearly with an increase of the external electric field that is in qualitative agreement with the experimental and numerical data presented in the literature. The effect of discharging of the second and third dust particles due to electrostatic lensing (ion focusing) on the first one was also demonstrated. The discharging occurs under the action of an additional ion flux due to the warping of ion trajectories by the potential of the dust particles in the chain. It is shown that for a certain large value of the external electric field, this effect is significant enough for the charge of the third dust particle to be the smallest of all the particles in the chain.

The presented model and the obtained results could be helpful in the study of the nature of self-organization of different ordered structures in strongly coupled Coulomb systems, and, in particular, in description of the formation of 1D chains (strings) or 2D–3D crystals of dust particles in low-temperature plasmas.

[1] J. H. Chu and Lin I, Direct Observation of Coulomb Crystals and Liquids in Strongly Coupled rf Dusty Plasmas, Phys. Rev. Lett. **72**, 4009 (1994).

[2] A. Melzer, T. Trottenberg, and A. Piel, Experimental determination of the charge on dust particles forming Coulomb lattices, Phys. Lett. A **191**, 301 (1994).

[3] H. Thomas, G. E. Morfill, V. Demmel, J. Goree, B. Feuerbacher, and D. Möhlmann, Plasma Crystal: Coulomb Crystallization in a Dusty Plasma, Phys. Rev. Lett. **73**, 652 (1994).

[4] V. E. Fortov, A. P. Nefedov, V. M. Torchinsky, V. I. Molotkov, O. F. Petrov, A. A. Samarian, A. M. Lipaev, and A. G. Khrapak, Crystalline structures of strongly coupled dusty plasmas in dc glow discharge strata, Phys. Lett. A **229**, 317 (1997).

[5] A. M. Lipaev, V. I. Molotkov, A. P. Nefedov, O. F. Petrov, V. M. Torchinskii, V. E. Fortov, A. G. Khrapak, and S. A. Khrapak, Ordered structures in a nonideal dusty glow-discharge plasma, J. Exp. Theor. Phys. **85**, 1110 (1997).

[6] A. V. Ivlev, M. H. Thoma, C. Räth, G. Joyce, and G. E. Morfill, Complex Plasmas in External Fields: The Role of Non-Hamiltonian Interactions, Phys. Rev. Lett. **106**, 155001 (2011).

[7] A. V. Zobnin, A. P. Nefedov, V. A. Sinel'shchikov, O. A. Sinkevich, A. D. Usachev, V. S. Filinov, and V. E. Fortov, Ordered dusty structures in the plasma of an RF electrodeless gas discharge, Plasma Phys. Rep. **26**, 415 (2000).

[8] M. Y. Pustylnik, M. A. Fink, V. Nosenko, T. Antonova, T. Hagl, H. M. Thomas, A. V. Zobnin, A. M. Lipaev, A. D. Usachev, V. I. Molotkov *et al.*, Plasmakristall-4: New complex (dusty) plasma laboratory on board the International Space Station, Rev. Sci. Instrum. **87**, 093505 (2016).

[9] O. Arp, J. Goree, and A. Piel, Particle chains in a dilute dusty plasma with subsonic ion flow, Phys. Rev. E **85**, 046409 (2012).

[10] K. Takahashi, T. Oishi, K.-i. Shimomai, Y. Hayashi, and S. Nishino, Analyses of attractive forces between particles in Coulomb crystal of dusty plasmas by optical manipulations, Phys. Rev. E **58**, 7805 (1998).

[11] A. Homann, A. Melzer, S. Peters, and A. Piel, Determination of the dust screening length by laser-excited lattice waves, Phys. Rev. E **56**, 7138 (1997).

[12] N. Sato, G. Uchida, T. Kaneko, S. Shimizu, and S. Iizuka, Dynamics of fine particles in magnetized plasmas, Phys. Plasmas **8**, 1786 (2001).

[13] C.-W. Io, C.-L. Chan, and Lin I, Cooperative microexcitations in 2+1D chain-bundle dusty plasma liquids, Phys. Plasmas **17**, 053703 (2010).

[14] E. A. Lisin, O. F. Petrov, E. A. Sametov, O. S. Vaulina, K. B. Statsenko, M. M. Vasiliev, J. Carmona-Reyes, and T. W. Hyde, Experimental study of the nonreciprocal effective interactions between microparticles in an anisotropic plasma, Sci. Rep. **10**, 13653 (2020).

[15] A. V. Ivlev, J. Bartnick, M. Heinen, C. R. Du, V. Nosenko, and H. Löwen, Statistical Mechanics where Newton's Third Law is Broken, Phys. Rev. X **5**, 011035 (2015).

[16] I. I. Lisina, E. A. Lisin, O. S. Vaulina, and O. F. Petrov, Coupling of dust particles in a weakly collisional plasma with an ion flow, J. Phys.: Conf. Ser. **1147**, 012112 (2019).

[17] P. Hartmann, M. Rosenberg, Z. Juhasz, L. S. Matthews, D. L. Sanford, K. Vermillion, J. Carmona-Reyes, and T. W. Hyde, Ionization waves in the PK-4 direct current neon discharge, Plasma Sources Sci. Technol. **29**, 115014 (2020).

[18] K. Vermillion *et al.*, Influence of temporal variations in plasma conditions on the electric potential near self-organized dust chains, Phys. Plasmas **29**, 023701 (2022).

[19] V. P. Yaroshenko and M. Pustylnik, Possible mechanisms of string formation in complex plasmas at elevated pressures, Molecules **26**, 308 (2021).

[20] L. S. Matthews *et al.*, Effect of ionization waves on dust chain formation in a dc discharge, J. Plasma Phys. **87**, 905870618 (2021).

[21] J. Kong, T. W. Hyde, L. Matthews, K. Qiao, Z. Zhang, and A. Douglass, One-dimensional vertical dust strings in a glass box, Phys. Rev. E **84**, 016411 (2011).

[22] T. W. Hyde, J. Kong, and L. S. Matthews, Helical structures in vertically aligned dust particle chains in a complex plasma, Phys. Rev. E **87**, 053106 (2013).

[23] J. Kong, K. Qiao, L. S. Matthews, and T. W. Hyde, Interaction force in a vertical dust chain inside a glass box, Phys. Rev. E **90**, 013107 (2014).

[24] M. Chen, M. Dropmann, B. Zhang, L. S. Matthews, and T. W. Hyde, Ion-wake field inside a glass box, Phys. Rev. E **94**, 033201 (2016).

[25] K. S. Ashrafi, R. Yousefi, M. Chen, L. S. Matthews, and T. W. Hyde, Dust as probes: Determining confinement and interaction forces, Phys. Rev. E **102**, 043210 (2020).

[26] R. Yousefi, M. Chen, L. S. Matthews, and T. W. Hyde, Charge of dust particles in a particle chain, arXiv:1607.03177.

[27] P. Ludwig, W. J. Miloch, H. Kählert, and M. Bonitz, On the wake structure in streaming complex plasmas, New J. Phys. **14**, 053016 (2012).

[28] W. J. Miloch and D. Block, Dust grain charging in a wake of other grains, Phys. Plasmas **19**, 123703 (2012).

[29] D. Block and W. J. Miloch, Charging of multiple grains in subsonic and supersonic plasma flows, Plasma Phys. Controlled Fusion **57**, 014019 (2015).

[30] D. Darian, W. J. Miloch, M. Mortensen, Y. Miyake, and H. Usui, Numerical simulations of a dust grain in a flowing magnetized plasma, Phys. Plasmas **26**, 043701 (2019).

[31] J. Schleede, L. Lewerentz, F. X. Bronold, R. Schneider, and H. Fehske, Plasma flow around and charge distribution of a dust cluster in a rf discharge, Phys. Plasmas **25**, 043702 (2018).

[32] L. S. Matthews, D. L. Sanford, E. G. Kostadinova, K. S. Ashrafi, E. Guay, and T. W. Hyde, Dust charging in dynamic ion wakes, Phys. Plasmas **27**, 023703 (2020).

[33] M. A. Lieberman and A. J. Lichtenberg, *Principles of Plasma Discharges and Materials Processing*, 2nd ed. (Wiley, New York, 2005).

[34] R. M. Roth, K. G. Spears, G. D. Stein, and G. Wong, Spatial dependence of particle light scattering in an rf silane discharge, Appl. Phys. Lett. **46**, 253 (1985).

[35] M. S. Barnes, J. H. Keller, J. C. Forster, J. A. O'Neill, and D. K. Coultas, Transport of Dust Particles in Glow-Discharge Plasmas, Phys. Rev. Lett. **68**, 313 (1992).

[36] G. I. Sukhinin, A. V. Fedoseev, T. S. Ramazanov, R. Z. Amangaliyeva, M. K. Dosbalayev, and A. N. Jumabekov, Nonlocal effects in a stratified glow discharge with dust particles, J. Phys. D: Appl. Phys. **41**, 245207 (2008).

[37] M. Salnikov, A. Fedoseev, and G. Sukhinin, Plasma parameters around a chain-like structure of dust particles in an external electric field, Molecules **26**, 3846 (2021).

[38] G. I. Sukhinin, A. V. Fedoseev, M. V. Salnikov, A. Rostom, M. M. Vasiliev, and O. F. Petrov, Plasma anisotropy around a dust particle placed in an external electric field, Phys. Rev. E **95**, 063207 (2017).

[39] V. E. Fortov, A. G. Khrapak, S. A. Khrapak, V. I. Molotkov, and O. F. Petrov, Dusty plasmas, Phys.-Usp. **47**, 447 (2004).

[40] C. Grossmann, H.-G. Roos, and M. Stynes, *Numerical Treatment of Partial Differential Equations* (Springer, Berlin, 2007), Vol. 154.

[41] M. Y. Pustylnik, A. A. Pikalev, A. V. Zobnin, I. L. Semenov, H. M. Thomas, and O. F. Petrov, Physical aspects of dust–plasma interactions, Contrib. Plasma Phys. **61**, e202100126 (2021).

[42] D. S. Lemons, M. S. Murillo, W. Daughton, and D. Winske, Two-dimensional wake potentials in sub- and supersonic dusty plasmas, Phys. Plasmas **7**, 2306 (2000).

[43] I. H. Hutchinson, Ion collection by a sphere in a flowing plasma: I. Quasineutral, Plasma Phys. Controlled Fusion **44**, 1953 (2002).

[44] G. A. Hebner and M. E. Riley, Structure of the ion wakefield in dusty plasmas, Phys. Rev. E **69**, 026405 (2004).

[45] R. Kompaneets, A. V. Ivlev, V. Nosenko, and G. E. Morfill, Wakes in inhomogeneous plasmas, Phys. Rev. E **89**, 043108 (2014).

[46] G. Sukhinin, M. Salnikov, A. Fedoseev, and A. Rostom, Plasma polarization and wake formation behind a dust particle in an external electric field, IEEE Trans. Plasma Sci. **46**, 749 (2018).

[47] S. A. Khrapak, A. V. Ivlev, G. E. Morfill, and H. M. Thomas, Ion drag force in complex plasmas, Phys. Rev. E **66**, 046414 (2002).

[48] S. A. Khrapak *et al.*, Particle charge in the bulk of gas discharges, Phys. Rev. E **72**, 016406 (2005).

[49] D. Samsonov and J. Goree, Instabilities in a dusty plasma with ion drag and ionization, Phys. Rev. E **59**, 1047 (1999).

[50] A. Piel *et al.*, Complex plasmas: Forces and dynamical behaviour, Plasma Phys. Controlled Fusion **50**, 124003 (2008).

[51] S. A. Khrapak, A. V. Ivlev, and G. E. Morfill, Momentum transfer in complex plasmas, Phys. Rev. E **70**, 056405 (2004).

[52] G. I. Sukhinin, M. V. Salnikov, and A. V. Fedoseev, The effect of the type of ion–neutral collisions on ion cloud formation, in *Diverse World of Dusty Plasmas: Proceedings of the 8th International Conference on the Physics of Dusty Plasmas*, AIP Conf. Proc. No. 1925 (AIP, Melville, NY, 2018), p. 020029.

[53] R. Le Picard and S. L. Girshick, The effect of single-particle charge limits on charge distributions in dusty plasmas, J. Phys. D: Appl. Phys. **49**, 095201 (2016).

[54] I. Goertz, F. Greiner, and A. Piel, Effects of charge depletion in dusty plasmas, Phys. Plasmas **18**, 013703 (2011).